Title

Adaptive Resistance to Dual BRAF/MEK Inhibition in BRAF-Driven Tumors through Autocrine FGFR Pathway Activation.

Journal

Clinical cancer research : an official journal of the American Association for Cancer Research, 25(23)

ISSN

1078-0432

Authors

Wang, Victoria E
Xue, Jenny Y
Frederick, Dennie T
et al.

Publication Date

2019-12-01

DOI

10.1158/1078-0432.ccr-18-2779

Peer reviewed

HHS Public Access

Author manuscript

Clin Cancer Res. Author manuscript; available in PMC 2020 June 01.

Published in final edited form as:

Clin Cancer Res. 2019 December 01; 25(23): 7202–7217. doi:10.1158/1078-0432.CCR-18-2779.

Adaptive Resistance to Dual BRAF/MEK Inhibition in BRAF-Driven Tumors Through Autocrine FGFR Pathway Activation

Victoria E. Wang[1,2], **Jenny Y. Xue**[3,9,10], **Dennie T. Frederick**[4], **Yi Cao**[5], **Eva Lin**[5], **Catherine Wilson**[5], **Anatoly Urisman**[2,7], **David P. Carbone**[8], **Keith T. Flaherty**[4], **Rene Bernards**[6], **Piro Lito**[3,9,10], **Jeff Settleman**[5,*], **Frank McCormick**[2,*]

[1]Department of Medicine, University of California, San Francisco, 94158, USA. [2]Helen Diller Comprehensive Cancer Center, University of California, San Francisco, 94158, USA. [3]Human Oncology and Pathogenesis Program, Memorial Sloan Kettering Cancer Center, New York, 10065, USA. [4]Massachusetts General Hospital Cancer Center, Boston, 02114, USA. [5]Discovery Oncology, Genentech, South San Francisco, 94080, USA. [6]Department of Molecular Carcinogenesis, Netherlands Cancer Institute, Netherlands. [7]Department of Pathology, University of California, San Francisco, 94158, USA. [8]The Ohio State University Comprehensive Cancer Center, Columbus, 43210, USA. [9]Weill Cornell/Rockefeller/Sloan Kettering Tri-Institutional MD-PhD Program, New York, NY, USA. [10]Weill Cornell Medical College, Cornell University, New York, New York, USA.

Abstract

Purpose: Combined mitogen-activated protein kinase (MAPK) pathway inhibition using dual BRAF and MEK inhibitors has prolonged the duration of clinical response in patients with $BRAF^{V600E}$ driven tumors compared to either agent alone. However, resistance frequently arises.

Experimental Design: We generated cell lines resistant to dual BRAF/MEK inhibition and utilized a pharmacological synthetic lethal approach to identify a novel, adaptive resistance mechanism mediated through the fibroblast growth factor receptor (FGFR) pathway.

Results: In response to drug treatment, transcriptional upregulation of FGF1 results in autocrine activation of FGFR, which sustains extracellular signal-regulated kinases (ERK) activation. FGFR inhibition overcomes resistance to dual BRAF/MEK inhibitors in both cell lines and patient derived xenograft (PDX) models. Abrogation of this bypass mechanism in the front-line setting enhances tumor killing and prevents the emergence of drug-resistant cells. Moreover, clinical data implicate serum FGF1 levels in disease prognosis.

[*]**Co-Corresponding Authors** Jeff Settleman, Pfizer, Inc., Science Center Drive, San Diego, CA 92121, Frank McCormick, UCSF Helen Diller Comprehensive Cancer Center, 1450 Third Street, San Francisco, CA 94158, Phone: (415)502-1710 FAX: (415)502-1712, Frank.mccormick@ucsf.edu.

Author contributions: VEW, YX, DTF, PL designed and performed experiments. YC provided guidance for sequencing analysis. EL and CW assisted with the screen, AU with histology. RB, KTF, PL provided clinical samples. RB, DPC, JS, FM provided input on experimental and study design. VEW wrote the manuscript with input from JS and FM. All authors read and approved the final manuscript.

Conflict of Interests: FM holds stock options in BridgeBio and sits on the advisory board of Daiichi Sankyo, Pfizer, and Amgen. KTF has served as a consultant to Novartis, Roche, and Array BioPharma and received research support from Novartis. EL, CW, and YC are employees of Roche/Genentech. JS is an employee of Pfizer.

Conclusions: Taken together, these results describe a new, adaptive resistance mechanism that is more commonly observed in the context of dual BRAF/MEK blockade as opposed to single agent treatment and reveal the potential clinical utility of FGFR targeting agents in combination with BRAF and MEK inhibitors as a promising strategy to forestall resistance in a subset of BRAF-driven cancers.

Keywords

Targeted therapy; BRAF and MEK inhibitors; FGF; resistance; cancer

Introduction

Oncogenic mutations affecting the BRAF serine/threonine kinase account for approximately 8% of all solid tumors, most commonly in melanoma but also in colorectal and lung adenocarcinomas, hairy-cell leukemia, and thyroid cancers [1-4]. Among the observed mutations, the $BRAF^{V600E}$ variant occurs most frequently across tumor types. This mutation promotes oncogenesis through hyperactivation of the MAPK pathway leading to uncontrolled cellular proliferation [5-7]. Targeted therapies using inhibitors directed against the mutated BRAF protein have dramatically improved survival. Clinical trials in selected patients using vemurafenib or dabrafenib (BRAF inhibitors) have yielded response rates (RR) in melanoma and non-small cell lung cancer (NSCLC) ranging from 33–53% [8-10]. Unfortunately, resistance to these targeted agents invariably occurs and limits their clinical efficacy over time. Numerous mechanisms of resistance to single agent BRAF inhibitors have been described, including 1) activation or mutations of alternative growth/survival pathways leading to downstream ERK activation such as oncogenic mutation in NRAS, NF1, COT, or increased PAK signaling [5, 7, 11-13], 2) mutations bypassing the original $BRAF^{V600E}$ such as splice variants and amplifications in the BRAF gene [14-16], or 3) paracrine activation of alternative signaling pathways such as the hepatocyte growth factor (HGF) [17, 18]. More recently, clinical trials utilizing dual MAPK blockade with the addition of MEK inhibitors have further extended the progression free survival (PFS) of these patients to a median of 11.4–12.25 months and RR ranging from 67–76% [19-22]. Even in the setting of combination therapy, resistance ultimately emerges, although the mechanisms of resistance to combination MAPK blockade remain less well-characterized [23-27].

Here we attempt to understand the mechanisms underlying resistance to combination BRAF/MEK inhibitors by adopting a pharmacological synthetic lethal screen in a panel of cancer cell lines that have been rendered resistant through long-term drug exposure. Our results revealed a novel reversible mechanism involving transcriptional feedback upregulation of the growth factor FGF1, which subsequently activates the FGFR cascade resulting in sustained ERK signaling.

Methods

Cell culture and reagents

Cell lines were obtained from the American Type Culture Collection (ATCC). All cells were cultured in RMPI-1640, supplemented with 10% FBS, penicillin/streptomycin, and L-glutamine and grown at 37°C in a humidified chamber with 5% CO_2. A375 parental and resistant lines were authenticated by short tandem repeat profiling. Cells were verified to be mycoplasma free (MycoAlert PLUS, Lonza). Chemical inhibitors were dissolved in DMSO for *in vitro* studies: vemurafenib (LC Labs), cobimetinib (MedChem Express), ponatinib (LC Labs), NVP-BGJ398 (MedChem Express), PD173074 (Selleckchem), dabrafenib (MedChem Express), and trametinib (LC Labs). A375 cells were treated with vemurafenib, cobimetinib or the combination starting at IC50 concentration and escalated weekly. Once resistant populations had been established, they were maintained at 2 μM for vemurafenib, 0.5 μM for cobimetinib, and 1.5/0.5 μM for the combination respectively.

Exome sequencing

Exon capture was performed using the Agilent SureSelect Human All Exon v5–51 Mb kit and the resulting libraries ran on HiSeq 2000. Average sequencing coverage was 106 x with an average of 5.6 Gbase per sample. The raw sequences were aligned to the human reference genome hg19 using the Burrows-Wheeler software. Variant calling was performed using Genome Analysis ToolKit in Galaxy. SNPs were compared to dbSNP, version 135, and In/Dels analyses were performed using PICARD, SAMTOOLS, and GATK. Variants derived from each resistant line were compared to the A375 parental. Sequencing data is available at the European Nucleotide Archive under the accession PRJEB34013.

Pharmacological synthetic lethal screen

1,500–2,000 cells were plated in 96 well plates. 24 hours later, the drug library, along with 1.5 μM and 0.5 μM cobimetinib, was dispensed into pre-specified wells using the Agilent Bravo Liquid Handling Platform. Viability was determined 72 hours after drug treatment using CellTiter-Glo (Promega). IC50 was determined using dose response curve fit in Prism. Each condition was run in triplicates.

Immunoblotting

Cells were lysed in RIPA buffer (ThermoFisher) containing protease inhibitors (Sigma P8340) and phosphatase inhibitor cocktails II and III (Sigma). Protein concentrations were quantitated using Bradford assay (Bio-Rad). SDS PAGE gel electrophoresis was used to separate the proteins (Invitrogen NuPAGE 4–12% Bis-Tris) in MOPS buffer. Resolved protein was transferred to nitrocellulose membranes (Invitrogen), blocked in 5% milk and probed using the following primary antibodies in either 5% milk or bovine serum albumin according to the manufacturer's protocol: PathScan Multiplex Western I (CST 5301), PD-L1 (CST 13684), pSTAT3 (CST 9145), pAxl (CST 5724), TAxl (CST 8661), MITF (CST 97800), pCRAF (CST 9427), pPAK1/PAK2 (CST 2606), pFGFR1 (CST 2544), and pFRS2- (CST 3861).

Cell proliferation assays

Cells were seeded at a density of 1 to 2 × 10^3 cells per well in 96-well plates. Drug treatment commenced 24 hours later at 10 μM with two-fold decrease dilution. After 72–96 hours of drug treatment, cellular proliferation was assessed using CellTiter-Glo (Promega). IC50s were determined using Prism (GraphPad). For colony formation assays, 10,000 cells were seeded in a 6-well plate and incubated with the appropriate drug for approximately two weeks. Media were changed every 4 to 6 days. Cells were then fixed with 4% formaldehyde and stained with 0.5% crystal violet, washed with distilled water, and photographed.

ELISA, conditioned media, and add-back assay

hFGF acidic ELISA was performed according to manufacturer's protocol (Raybiotech ELH-aFGF-1). Serum was diluted 2 fold prior to testing. For conditioned media experiment, 1 × 10^6 cells were plated on a 10 cm plate with 2% FBS in the presence and absence of the BRAF/MEK combination. After 72 hours, media was replaced, collected after an additional 24, 48 hours, and 1 week, and spun down for 10 minutes at 300 RCF. Drug naïve cells were plated in 96 well plates at a density of 1 to 2 × 10^3 cells per well with conditioned media. Exogenous growth factors were added at 50 ng/mL to cells in 96 well plates. For the neutralizing assay, a polyclonal antibody (Abcam 9588) to FGF1 was added to the conditioned media at 10 μg/mL and incubated for 30 minutes to 1 hour prior to performing the cell viability assay in 96 well plates described above. A polyclonal IgG isotype control (Abcam 37415) was used in parallel. Cell viability was assayed after 72 hours utilizing CellTiter-Glo.

Tumor xenograft studies and immunohistochemistry

Xenograft studies were approved by the UCSF Animal Care and Use Committee. A375 parental and A375 VCR cells were injected subcutaneously into both flanks of 6 weeks old NCr nude mice (Taconic) at a concentration of 2 × 10^6/200 μL in Matrigel (354234). Each arm of the study included 5 mice (10 tumors per treatment group). When tumors reached ~100 mm^3, as determined by an electronic caliper, the animals were randomized depending on the study. For the pilot study, animals were randomized into two groups, each receiving either vehicle or vemurafenib 25 mg/kg and cobimetinib 4 mg/kg dissolved in 5% DMSO, 30% PEG300, and 5% Tween 80 by oral gavage daily. A375 VCR xenografts were randomized into four groups receiving either vehicle, ponatinib 20 mg/kg dissolved in 5% DMSO, 30% PEG300, and 5% Tween 80, vemurafenib 25 mg/kg and cobimetinib 4 mg/kg, or the triple combination via oral gavage daily. Tumors and body weight were measured twice a week.

Tumor samples were harvested postmortem and fixed in formalin for 72 hours and then placed in 70% ethanol for 24 hours prior to embedding in paraffin. Samples were sectioned via microtome at a thickness of 5 microns. Immunohistochemistry was performed by HistoWiz Inc. on a Bond Rx autostainer (Leica) with enzyme treatment (1:1,000) using standard protocols. Antibodies used were pERK (CST 4370 1:1,000) and Ki67 (Leica PA0230). Bond Polymer Refine Detection (Leica) was used according to manufacturer's protocol. Whole slide scanning (40x) was performed on an Aperio AT2 (Leica). The images

were quantified using Halo Image analysis software (Indica Labs) using CytoNuclear module.

Patient specimen collection and RNA sequencing

Clinical data and tissue collection from patients with BRAF melanoma and NSCLC was performed with informed consent of patients at the Netherland Cancer Institute, Massachusetts General Hospital, or Memorial Sloan Kettering, in accordance with the Institutional Review Boards at these institutions and the US Common Rule. RNA was isolated from FFPE samples as described previously [28, 29]. For RNA sequencing, the library was prepared using TruSeq RNA sample prep kit according to the manufacturer's protocol (Illumina). Paired-end 2 × 75 bp sequencing was performed using Illumina HiSeq 2000. RNA sequencing data are available at http://www.ncbi.nlm.nih.gov under accession number GSE50535 and the European Genome-phenome Archive (EGA S00001000992).

Results

Generation and characterization of $BRAF^{V600E}$ cell lines resistant to dual MAPK blockade

To model mechanisms of acquired resistance of $BRAF^{V600E}$ driven tumors to dual BRAF/MEK inhibition, cell lines were generated from A375 human melanoma cells harboring the $BRAF^{V600E}$ mutation using escalating doses of vemurafenib (A375 VemR), cobimetinib (A375 CobiR), or the combination (A375 VCR) (Fig. 1a). Viability without any drug added was normalized to be one hundred percent. These cells also demonstrate resistance to other BRAF and MEK inhibitors such as dabrafenib and trametinib (Fig. S1a). A375-VemR cells were resistant to BRAF inhibitors only but remained sensitive to MEK and ERK inhibitors, suggesting that the resistance mechanism lies at the level of RAF (Fig. 1a). In contrast, A375-CobiR cells exhibited resistance to both BRAF and MEK inhibitors but remained sensitive to ERK inhibition. Therefore, the resistance mechanism likely lies downstream of BRAF but upstream of ERK. The dual-resistant A375 VCR cells showed strong resistance to all agents tested, including ~ 100 fold increase in resistance to single agent vemurafenib or cobimetinib compared to the parental cells and a greater than 10 fold increase in resistance to the combination and to ERK inhibition, suggesting either an on-target mutation of ERK or a bypass track resulting in ERK activation. Both A375-VemR and A375-CobiR remained resistant to the drug even after a prolonged drug holiday. Upon cessation of drug treatment, however, the growth rate of A375 VCR slowed and these cells became re-sensitized to the drugs after three weeks of drug holiday (Fig. S1b). Exome sequencing of the A375 VemR and A375 CobiR cells revealed previously described resistance-associated mutations in NRAS and MEK1 respectively (Table S1-3) [7, 23]. However, no driver mutations or genomic amplifications were identified for the dual-resistant A375 VCR line. Immunoblotting of the A375 VCR cells showed elevated pAKT, pSTAT3, and persistent pERK activation despite treatment with BRAF/MEK inhibitors (Fig. 1b). All of these cells exhibited robust MITF expression. pCRAF levels were increased in the resistant lines but contrary to previous reports, pPAK1/2 levels was only mildly increased in this model [12]. At baseline, A375 cells express high levels of PD-L1, which is abolished upon inhibition of the MAPK pathway, consistent with prior reports that oncogenic signaling may trigger immune escape by inhibiting antitumor immunity [30]. Since pSTAT3 has

previously been implicated as a resistance mechanism in several different tumors, we tested whether STAT3 loss of function would re-sensitize the cells to the combination treatment and gain of function would confer resistance [31]. Targeting STAT3 using siRNAs did not alter sensitivity to MAPK blockade in the A375 VCR resistant cells (Fig. S1c and S1d); neither did constitutive overexpression of STAT3 using a lentiviral construct (Fig. S1d). Together, these data suggest that resistance of the A375 VCR cells was likely mediated through a STAT3-independent compensatory pathway resulting in sustained ERK or AKT activation.

Pharmacological synthetic lethal screen to identify pathways mediating resistance to dual MAPK inhibition

To identify the pathway(s) mediating resistance in the A375 VCR cells, a pharmacological screen was conducted using an 86 compound library that targeted kinases, epigenetic regulators, metabolic enzymes, and apoptosis regulators (Table S4). Several chemotherapeutic agents and antibody-drug conjugates were also included. Each drug was tested under three conditions: A375 parental, A375 VCR, and A375 VCR in the presence of vemurafenib and cobimetinib. Targets of interest synergized with BRAF/MEK inhibition to selectively enhance killing of the A375 VCR cells while having minimal effect on the viability of parental or resistant cells in the absence of BRAF and MEK inhibitors (Fig. 1c). For each compound tested, the IC50 ratio of the parental line treated with drug X versus the resistant line treated with drug X plus BRAF/MEK inhibitors (IC50 1) and the ratio of the resistant line treated with drug X versus with dual inhibitors and drug X (IC50 2) served as the activity readouts of the agent in question to promote cellular killing. Compounds that exhibited low IC50 1 but high IC50 2 ratios served as proof-of-concept controls. This class included MAPK inhibitors capable of killing parental A375 cells as a single agent, but not the A375 VCR cells. Molecules that synergized with the BRAF/MEK combination to promote selective killing of the resistant population displayed both high IC50 1 and IC50 2 ratios (Fig. 1d). Broadly defined, these agents fall into several pharmacological categories: PI3K/AKT inhibitors, Src inhibitors, and potential novel targets including CHK1, BTK, and FGFR inhibitors (Table S4). Antibody drug conjugates and chemotherapy differentially enhanced killing of the resistant cells in the presence of the drug combination without affecting the parental cells. Consistent with our prior observations, STAT3 inhibitors did not synergize with dual MAPK inhibition.

Activation of FGFR is a bypass mechanism to activate ERK

Top hits from the screen were re-tested in a 72 hour viability assay (Fig. 2a and S1e). Cells treated with the relevant drugs were also tested for apoptosis using the Caspase Glo assay. Staurosporine serves as a positive control, and staurosporine treated cells (1 μM) all exhibit high levels of apoptosis. As expected, vemurafenib and/or cobimetinib induced apoptosis in the A375 parental cells but not in the A375 VCR cells. Addition of ponatinib to the combination induced higher level of cell death in the A375 VCR cells (Fig. S1f). Since PI3K/AKT and Src inhibitors have previously been reported to overcome resistance to MAPK inhibition, we focused on the novel targets. Ponatinib, an inhibitor of multiple kinases including Bcr-Abl, PDGFR, VEGFR2, FGFR1, c-Src, and c-Kit, was the highest scoring hit based on both IC50 1 and 2 that is not an exclusive PI3K/AKT or Src inhibitor.

Since multiple downstream effectors, including pSTAT3 and pAKT, appeared to be activated in the A375 VCR cells, we hypothesized that the resistance mechanism is likely mediated through upstream receptor activation and we therefore tested several more specific FGFR inhibitors. Both NVJ-BGJ398 (a FGFR1/2/3 inhibitor) and PD173074 (a selective FGFR1 inhibitor) enhanced A375 VCR tumor killing with the BRAF/MEK inhibitor combination in both short-term viability assays and long-term colony formation studies while having minimal perturbation on the survival of A375 parental and A375 VCR cells in the absence of the BRAF/MEK combination (Fig. 2a and b). In comparison, the selective FGFR4 inhibitor, BLU554, did not augment tumor killing. A second, independently generated dual resistant cell line, Mel888 DR, also exhibited increased sensitivity to ponatinib compared to the parental Mel888 cells (Fig. 2a). This cell line has been previously described as being highly resistant to dabrafenib and trametinib, which was confirmed in our assay. Similar to the observation in A375 VCR cells, both ponatinib and NVJ-BGJ398 increased killing Mel888 DR cells in the presence of dabrafenib and trametinib (Fig. 2b). Taken together, we conclude that the mechanism mediating resistance of the dual resistant population most likely involves compensatory FGFR1 activation.

To elucidate the biochemical consequences of FGFR blockade on the A375 VCR cells, immunoblotting was performed after escalating doses of ponatinib, either as a single agent or in combination with fixed doses of vemurafenib and cobimetinib. With the triple combination, there was a striking decrease in the level of pERK, a finding that was also recapitulated with NVJ-BGJ398 and PD173074 treatments but not with the FGF4 selective inhibitor (Fig. 2c and Fig. S2a). Suppression of pERK in the A375 parental and A375 VCR cells at the drug concentrations used occurred by two hours whereas suppression of pFGFR occurred between four to six hours. Twenty-four hours after drug treatment, pFGFR was completely suppressed, and pERK appeared diminished in the A375 VCR cells even with single agent ponatinib treatment (Fig. S1g). Similarly, treatment with dabrafenib, trametinib, and ponatinib potently suppressed pERK and pFGFR in Mel888 DR cells (Fig. S1h). Interestingly, treatment with ponatinib did not alter protein levels of other downstream effectors such as pSTAT3 and pAKT.

Dual BRAF/MEK inhibition results in transcriptional activation of FGF1 and FGFR activation

We hypothesized that there may be one or more survival factor(s) secreted by the tumor cells in response to drug treatment serving to activate a signaling pathway, as reported previously by other groups [17, 18, 32]. To test this hypothesis, conditioned media from both A375 parental and A375 VCR cells pre- and post-drug treatment were harvested. The media was subsequently tested on drug naïve, parental A375 cells in the presence of escalating doses of vemurafenib and cobimetinib. Post-drug- treated media conferred resistance to the BRAF/MEK inhibitor combination compared to the control, suggesting the presence of soluble factors promoting cellular survival (Fig. 3a). The ability of the conditioned media to confer resistance is “extinguishable” over time after drug withdrawal (Fig. 3a and Fig. S2b).

To identity this factor or combination of factors, a targeted growth factor real-time PCR array was utilized to compare differential gene expression pre- and post-drug treatment. In

both drug-treated A375 and Mel888 parental and dual resistant A375 VCR and Mel888 DR cells, only a few select FGFs are transcriptionally upregulated in response to dual MAPK inhibition including FGF1, FGF7, FGF14, and FGF17 (Fig. 3b). The landscape of upregulated FGF factors is similar across both cell lines. Addition of each of these factors to the drug naïve A375 parental cells treated with the BRAF/MEK inhibitor combination showed that only FGF1 was able to confer significant resistance, by over ten fold, whereas FGF7 and FGF17 did not confer any appreciable resistance (Fig. 3c). Furthermore, exogenous treatment with FGF1 resulted in increased level of pFGFR1 and signaling through this pathway (Fig. 3c). Consistent with this, the media showed a three-fold increase in FGF1 levels after treatment with the drug combination compared with the pre-treatment control (Fig. 3d). In contrast, there was no increase in the A375 CobiR and a less prominent increase in the A375 VemR samples (Fig. S2c), likely due to the fact that these cells are driven by acquired mutations rather than a non-genetic, compensatory signaling mechanism. Depletion of FGF1 using a neutralizing antibody diminished the ability of the conditioned media from drug-treated cells to promote resistance in drug-naïve cells (Fig. 3e). We extended this analysis to a larger panel of cells lines harboring the $BRAF^{V600E}$ mutation, including HCC364, a lung cancer cell line dependent on BRAF. In most of the cell lines where FGF1 was able to promote drug resistance (MALME-3M, LOX-IMVI, 1205-LU, HCC364, and UACC-62), FGF1 RNA was increased by at least three fold in response to dual vemurafenib and cobimetinib treatment for 72 hours (Fig. 4a and 4b). There was a concomitant increase in FGF1 levels detectable in the media within 72 hours post-drug treatment (Fig. 4c), suggesting that this phenomenon might be broadly applicable to subsets of BRAF-driven tumors. Conversely, cell lines in which resistance was not induced by addition of FGF1 in response to BRAF/MEK inhibition did not demonstrate any appreciable change in FGF1 levels in the media from drug- treated cells (SK-MEL 28 and WM-164) (Fig. 4b and 4c). Furthermore, upregulation of FGFR is specifically observed in the dual-resistant A375 VCR cells (Fig. 4d). These cells appear to rely primarily on FGFR, the insulin receptor, and to a lesser extent, PDGFR, although one cannot definitely conclude whether this is due to hyperactivation of parallel signaling pathways within the same clone or coexistence of multiple clones, each with unique RTK dependency. In contrast, the A375 parental, VemR, and CobiR exhibit elevated EGFR and HGFR/c-Met signaling as previously reported [33] [17] [18]. Taken together, these results indicate that tumor cells transcriptionally upregulate pro-survival mediators, such as FGF1, after exposure to drug, and these factors subsequently enhance tumor survival in an autocrine manner through activation of downstream signaling pathways.

Co-Targeting with FGFR pathway inhibitors re-sensitizes tumors to dual BRAF/MEK inhibition and delays the emergence of resistance

To establish the physiological relevance of our findings, xenograft models were established using A375 parental and VCR lines. Pilot experiments wherein A375 parental xenografts were treated with vemurafenib 25 mg/kg and cobimetinib 4 mg/kg daily via oral gavage resulted in significant decrease in tumor volume (Fig. S3a). Toxicity was minimal as assessed by body weight (Fig. S3b). Immunohistochemistry on tumor sections verified decreased pERK expression (Fig. S3c). In a four-arm study, the A375 VCR xenografts were treated with vehicle, ponatinib at 20 mg/kg, dual vemurafenib and cobimetinib (25 mg/kg

and 4 mg/kg respectively), or the triple combination including ponatinib. The triple combination arm showed significant tumor regression compared with the other three arms (Fig. 5a) with virtually no difference in body weight alterations over time (Fig. S3d). Similarly, Mel888DR xenografts treated with the triple combination had significantly smaller tumor volume compared with those treated with vemurafenib and cobimetinib (25 mg/kg and 4 mg/kg respectively) (Fig. 5g). Tumors in the dual combination arm grew after approximately fourteen days, though interestingly, tumors in the vehicle and single agent ponatinib-treated animals remained static, which may be related to oncogene-induced senescence upon withdrawal of the inhibitors as reported previously [28]. The animals in the vemurafenib and cobimetinib arm were subsequently re-randomized to either continuing on the combination or to addition of ponatinib (Fig. 5b). Results indicated that sequential addition of ponatinib reduced tumor volume compared to those animals that continued on the dual combination therapy with a slight decrement in weight, although this observation can be attributed at least in part due to the rapidly enlarging tumor volume in the dual combination animals rather than treatment induced cachexia (Fig. S3e). In addition to inducing tumor regression in the dual resistant A375 VCR cells, addition of FGFR blockade upfront in drug-naïve parental cells delayed the emergence of resistance without evidence of toxicity both *in vitro* and in xenograft models (Fig. 5c, 5d, and Fig. S3f). Consistent with our results *in vitro*, the triple combination inhibited pERK and exhibited decreased Ki-67 expression (a marker of cellular proliferation) in immunohistochemical studies compared to the other arms (Fig. 5e). Serum level of FGF1 harvested from A375 parental xenografts was also higher after drug treatment (Fig. 5f).

FGF1 is transcriptionally up-regulated in melanoma and NSCLC progression tumor samples and portends a worse prognosis

To determine if any of the FGF genes identified by our functional approach might promote clinical resistance to MAPK inhibitors, we obtained RNA sequencing data from paired biopsies of melanoma and NSCLC patients, two tumor types where BRAF mutations occur at an appreciable frequency (35–50% and 5–8% respectively). All patients underwent a biopsy prior to treatment initiation and then either while on treatment or at the time of disease progression. Among the four NSCLC patients, all of whom received the BRAF/MEK combination, two demonstrated an increase in FGF1 expression at progression, one without change, and one showed a decrease in FGF1 levels (Fig. 6a). Progression biopsy harvested from patient one, who had been treated with dabrafenib and trametinib and exhibited elevated FGF1 levels, was used to generate a patient derived xenograft (PDX) model. These animals were subsequently treated with vemurafenib and cobimetinib or the triple combination including ponantinib. The triple combination arm exhibited reduced tumor growth compared to the vemurafenib and cobimentinib combination (Fig. 6b).

Out of twenty melanoma patients, nine received a single agent BRAF inhibitor while eleven were treated with the BRAF/MEK inhibitor combination. Only one out of nine patients (22%) treated with a BRAF inhibitor demonstrated an increase of FGF1 levels post-treatment by more than twofold. In contrast, six out of eleven patients (55%) who received the combination had post-treatment FGF1 levels of greater than twofold (Fig. 6c). The mean overall survival was markedly worse amongst the seven patients whose post-treatment FGF1

increased by more than twofold, regardless of the treatment received, compared to those who did not (15.27 months versus 71.44 months, p = 0.037). Furthermore, all four patients who were alive at the time of censoring were FGF1 low (Fig. 6d).

Discussion

Implementing a pharmacological synthetic lethal screen using a reversibly resistant $BRAF^{V600E}$ driven cell line, we identified a novel mechanism underlying drug resistance to combination BRAF/MEK therapies, providing insight into a signaling network rewiring in the dual resistant population. Upon initial cytotoxic insult with the drug combination, the majority of treatment naive cells will undergo apoptosis. However, a small fraction of the tumor cells capable of transcriptionally upregulating growth factors such as FGF1 may survive the initial drug onslaught, possibly reflecting heterogeneity of chromatin states among the cellular population. This subset of therapy-induced persister cells *in vitro* appears to recapitulate the state of residual disease *in vivo* that resumes proliferation over time leading to disease recurrence either through the development of secondary mutations or, as in our model, by co-opting the transcriptional activation of growth factors to ensure its long-term survival. In our system, both the parental A375 drug treated and A375 VCR cells exhibited higher FGF1 levels relative to the parental non-drug treated cells. After prolonged exposure to the drug combination, however, the A375 VCR cells showed lower FGF1 expression compared to the parental A375 cells treated acutely with the drug combination, suggesting a potential feedback mechanism of FGF1 regulation that remains to be identified.

Our data suggest that FGF1 activation is an important mediator of cellular survival in a subset of $BRAF^{V600E}$ driven melanomas and NSCLCs treated with the BRAF/MEK inhibitor combination. To this end, abrogation of this feedback response with the addition of FGFR-directed therapy upfront may decrease the number of persister cells and ultimately delay the emergence of resistant clones. The concept of an autocrine circuit involving a secreted factor that subsequently activates a pro-survival receptor tyrosine kinase pathway has been described in other tumor resistance models including AML, and EGFR- and ALK-driven NSCLC [32, 34]. Furthermore, our findings substantiate prior reports whereby FGFR3 activation confers resistance to vemurafenib *in vitro* [35] and that feedback activation of FGFR1 served as an adaptive resistance mechanism in KRAS-mutated lung cancers after MEK inhibition [36], implicating the FGFR feedback loop as a broad resistance mechanism in various tumor types. Consistent with our findings, MEK inhibition increased FRS2, pERK and pAKT levels but addition of ponatinib blunted these responses. However, FGFR inhibition is unlikely to be successful in BRAF or KRAS driven colorectal cancer models since these tumors appear to rely largely on EGFR activation as the prominent feedback mechanism, demonstrating important tumor-specific differences [37]. A recent report has shown increased PAK signaling as an important response to MAPK inhibitors [12]. While we did not observe substantial increase of pPAK in our dual resistant population (Fig. 1b), one of the cell lines that demonstrated high levels of PAK expression in response to MAPK inhibitors was WM-164 which, interestingly, did not respond to exogenous stimulation by FGF1 (Supplementary Fig. 2d). This may represent an example of tumor heterogeneity whereby tumor cells evolve parallel pathways to circumvent resistance.

Understanding and predicting the feedback mechanism utilized by the tumor cells would be highly informative for precision deployment of rational drug combinations.

Even after prolonged exposure to the BRAF/MEK combination, no acquired resistance mutations were detected in the dual resistant population. By comparison, acquired resistance mutations in NRAS and MEK1 emerged relatively rapidly in each of the single treatment arms, likely because the combination treatment presented a higher fitness threshold. Because of the fitness disadvantage conferred by combination therapy, subclones with acquired mutations never propagate sufficiently to reach a detectable level within the tumor population [38]. As a result, these tumor cells may preferentially hyperactivate a compensatory growth signaling pathway in order to surpass this fitness threshold. This observation is supported by our clinical data, since patients who received dual BRAF and MEK inhibitors exhibit a strikingly higher frequency of upregulated FGF1 expression compared to those who received single agent therapy. Furthermore, patients who displayed increased intratumoral FGF1 mRNA levels in response to MAPK inhibition had a worse overall survival. This result, coupled with elevated serum FGF1 levels detected after dual MAPK inhibition, raises the possibility that FGF1 may serve as a prognostic marker for disease survival in BRAF-driven melanomas and as a predictive marker identifying the subset of patients who may benefit from the addition of a FGFR inhibitor. It is also interesting to note that ponatinib has a lower IC50 compared with the more specific FGFR inhibitors. This may be due to the more promiscuous nature of ponatinib and its additional inhibitory activity on PDGFR and Src. Taken together, our data suggest that 1) clinical deployment of FGFR directed therapy may be a strategy to re-sensitize a broad range of resistant tumor cells after MAPK blockade, and that 2) inhibiting multiple signaling pathways using low dose combination therapies upfront may augment the killing of tumor persister cells and prevent the emergence of a resistant population by targeting multiple subclones present at low frequencies.

Clinical deployment of the rational combination to include a FGFR inhibitor in addition to dual BRAF and MEK inhibitors in phase I clinical trials is warranted in $BRAF^{V600E}$ driven melanoma and NSCLC to test for safety and efficacy. Future work should be directed to the prediction of feedback mechanisms likely to be utilized by resistant tumors, and an understanding of why certain pathways are preferentially selected in patients over others, with the goal of improving rational drug combinations. Additional studies are also needed to understand how the autocrine secretome contributes to the establishment and maintenance of a tumorigenic niche, as well as its effect on tumor stromal cells and the immune microenvironment.

Supplementary Material

Refer to Web version on PubMed Central for supplementary material.

Acknowledgments:

We thank members of the McCormick laboratory for helpful discussions and input and Andrew Wolfe for critical reading of the manuscript.

Funding: This research was supported by a Damon Runyon Postdoctoral Award to VEW (121570), an ASCO Young Investigator Award to VEW (P0511381), a Lung Cancer Research Foundation Fellowship to VEW (LC170486), and Department of Defense Career Development Award (W81XWH-17-1-0365, W81XWH-18-1-0551) to VEW. PL is supported in part by the NIH/NCI (1R01CA23074501, 1R01CA23026701A1) and The Pew Charitable Trusts.

References

1. Davies H, et al., Mutations of the BRAF gene in human cancer. Nature, 2002 417(6892): p. 949–54. [PubMed: 12068308]
2. Hodis E, et al., A landscape of driver mutations in melanoma. Cell, 2012 150(2): p. 251–63. [PubMed: 22817889]
3. Hyman DM, et al., Vemurafenib in Multiple Nonmelanoma Cancers with BRAF V600 Mutations. N Engl J Med, 2015 373(8): p. 726–36. [PubMed: 26287849]
4. Tiacci E, et al., Targeting Mutant BRAF in Relapsed or Refractory Hairy-Cell Leukemia. N Engl J Med, 2015 373(18): p. 1733–47. [PubMed: 26352686]
5. Johannessen CM, et al., COT drives resistance to RAF inhibition through MAP kinase pathway reactivation. Nature, 2010 468(7326): p. 968–72. [PubMed: 21107320]
6. Lito P, et al., Relief of profound feedback inhibition of mitogenic signaling by RAF inhibitors attenuates their activity in BRAFV600E melanomas. Cancer Cell, 2012 22(5): p. 668–82. [PubMed: 23153539]
7. Nazarian R, et al., Melanomas acquire resistance to B-RAF(V600E) inhibition by RTK or N-RAS upregulation. Nature, 2010 468(7326): p. 973–7. [PubMed: 21107323]
8. Sosman JA, et al., Survival in BRAF V600-mutant advanced melanoma treated with vemurafenib. N Engl J Med, 2012 366(8): p. 707–14. [PubMed: 22356324]
9. Planchard D, et al., Dabrafenib in patients with BRAF(V600E)-positive advanced non-small-cell lung cancer: a single-arm, multicentre, open-label, phase 2 trial. Lancet Oncol, 2016 17(5): p. 642–50. [PubMed: 27080216]
10. Chapman PB, et al., Improved survival with vemurafenib in melanoma with BRAF V600E mutation. N Engl J Med, 2011 364(26): p. 2507–16. [PubMed: 21639808]
11. Lito P, Rosen N, and Solit DB, Tumor adaptation and resistance to RAF inhibitors. Nat Med, 2013 19(11): p. 1401–9. [PubMed: 24202393]
12. Lu H, et al., PAK signalling drives acquired drug resistance to MAPK inhibitors in BRAF-mutant melanomas. Nature, 2017.
13. Whittaker SR, et al., A genome-scale RNA interference screen implicates NF1 loss in resistance to RAF inhibition. Cancer Discov, 2013 3(3): p. 350–62. [PubMed: 23288408]
14. Poulikakos PI, et al., RAF inhibitor resistance is mediated by dimerization of aberrantly spliced BRAF(V600E). Nature, 2011 480(7377): p. 387–90. [PubMed: 22113612]
15. Shi H, et al., Acquired resistance and clonal evolution in melanoma during BRAF inhibitor therapy. Cancer Discov, 2014 4(1): p. 80–93. [PubMed: 24265155]
16. Lin L, et al., Mapping the molecular determinants of BRAF oncogene dependence in human lung cancer. Proc Natl Acad Sci U S A, 2014 111(7): p. E748–57. [PubMed: 24550319]
17. Straussman R, et al., Tumour micro-environment elicits innate resistance to RAF inhibitors through HGF secretion. Nature, 2012 487(7408): p. 500–4. [PubMed: 22763439]
18. Wilson TR, et al., Widespread potential for growth-factor-driven resistance to anticancer kinase inhibitors. Nature, 2012 487(7408): p. 505–9. [PubMed: 22763448]
19. Flaherty KT, et al., Combined BRAF and MEK inhibition in melanoma with BRAF V600 mutations. N Engl J Med, 2012 367(18): p. 1694–703. [PubMed: 23020132]
20. Johnson DB, et al., Combined BRAF (Dabrafenib) and MEK inhibition (Trametinib) in patients with BRAFV600-mutant melanoma experiencing progression with single-agent BRAF inhibitor. J Clin Oncol, 2014 32(33): p. 3697–704. [PubMed: 25287827]
21. Larkin J, et al., Combined vemurafenib and cobimetinib in BRAF-mutated melanoma. N Engl J Med, 2014 371(20): p. 1867–76. [PubMed: 25265494]

22. Long GV, et al., Combined BRAF and MEK inhibition versus BRAF inhibition alone in melanoma. N Engl J Med, 2014 371(20): p. 1877–88. [PubMed: 25265492]
23. Emery CM, et al., MEK1 mutations confer resistance to MEK and B-RAF inhibition. Proc Natl Acad Sci U S A, 2009 106(48): p. 20411–6. [PubMed: 19915144]
24. Johannessen CM, et al., A melanocyte lineage program confers resistance to MAP kinase pathway inhibition. Nature, 2013 504(7478): p. 138–42. [PubMed: 24185007]
25. Konieczkowski DJ, et al., A melanoma cell state distinction influences sensitivity to MAPK pathway inhibitors. Cancer Discov, 2014 4(7): p. 816–27. [PubMed: 24771846]
26. Lin L, et al., The Hippo effector YAP promotes resistance to RAF- and MEK-targeted cancer therapies. Nat Genet, 2015 47(3): p. 250–6. [PubMed: 25665005]
27. Moriceau G, et al., Tunable-combinatorial mechanisms of acquired resistance limit the efficacy of BRAF/MEK cotargeting but result in melanoma drug addiction. Cancer Cell, 2015 27(2): p. 240–56. [PubMed: 25600339]
28. Sun C, et al., Reversible and adaptive resistance to BRAF(V600E) inhibition in melanoma. Nature, 2014 508(7494): p. 118–22. [PubMed: 24670642]
29. Kwong LN, et al., Co-clinical assessment identifies patterns of BRAF inhibitor resistance in melanoma. J Clin Invest, 2015 125(4): p. 1459–70. [PubMed: 25705882]
30. Akbay EA, et al., Activation of the PD-1 pathway contributes to immune escape in EGFR-driven lung tumors. Cancer Discov, 2013 3(12): p. 1355–63. [PubMed: 24078774]
31. Lee HJ, et al., Drug resistance via feedback activation of Stat3 in oncogene-addicted cancer cells. Cancer Cell, 2014 26(2): p. 207–21. [PubMed: 25065853]
32. Kentsis A, et al., Autocrine activation of the MET receptor tyrosine kinase in acute myeloid leukemia. Nat Med, 2012 18(7): p. 1118–22. [PubMed: 22683780]
33. Girotti MR, et al., Inhibiting EGF receptor or SRC family kinase signaling overcomes BRAF inhibitor resistance in melanoma. Cancer Discov, 2013 3(2): p. 158–67. [PubMed: 23242808]
34. Obenauf AC, et al., Therapy-induced tumour secretomes promote resistance and tumour progression. Nature, 2015 520(7547): p. 368–72. [PubMed: 25807485]
35. Yadav V, et al., Reactivation of mitogen-activated protein kinase (MAPK) pathway by FGF receptor 3 (FGFR3)/Ras mediates resistance to vemurafenib in human B-RAF V600E mutant melanoma. J Biol Chem, 2012 287(33): p. 28087–98. [PubMed: 22730329]
36. Manchado E, et al., A combinatorial strategy for treating KRAS-mutant lung cancer. Nature, 2016 534(7609): p. 647–51. [PubMed: 27338794]
37. Prahallad A, et al., Unresponsiveness of colon cancer to BRAF(V600E) inhibition through feedback activation of EGFR. Nature, 2012 483(7387): p. 100–3. [PubMed: 22281684]
38. Xue Y, et al., An approach to suppress the evolution of resistance in BRAFV600E-mutant cancer. Nat Med, 2017 23(8): p. 929–937. [PubMed: 28714990]

Translational Relevance: The recent approval of the BRAF/MEK inhibitor combination by the FDA in a variety of BRAF driven malignancies has highlighted the clinical problem of drug resistance and the urgent need for patients who progress on combination therapy. Here, we describe transcriptional upregulation of FGF1 as a feedback mechanism that confers adaptive resistance to BRAF/MEK therapy and contributes to the formation of persister cells after drug therapy. Elevated serum FGF1 after MAPK inhibition serves as a potential biomarker for patient identification. Addition of an FGFR inhibitor overcame resistance to dual BRAF/MEK inhibition and delayed the emergence of resistance when used in the frontline setting. Thus, the triple combination may warrant clinical testing in patients with BRAF driven malignancies.

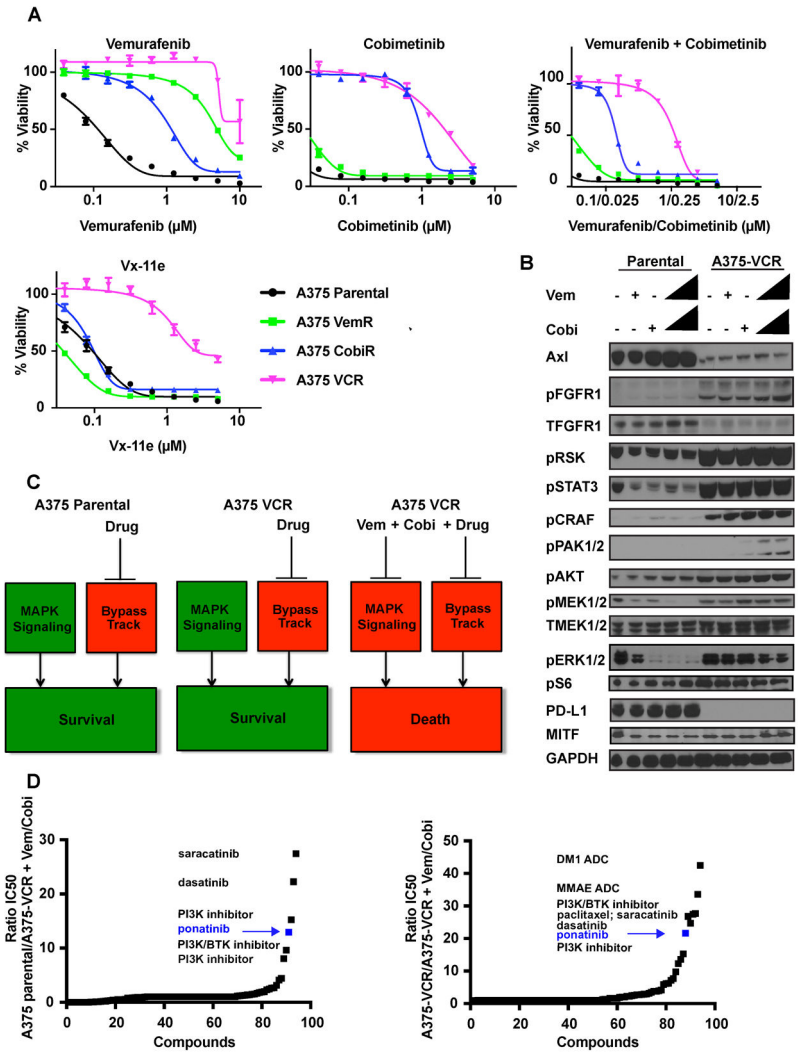

Figure 1. Pharmacological synthetic lethal screen to identify resistance mechanism to dual BRAF and MEK inhibition.

(A) Drug sensitivity profile of A375 resistant lines generated by escalating drug dosage to BRAF (vemurafenib), MEK (cobimetinib), and ERK (Vx-11e) inhibitors. Cell proliferation was quantitated by CellTiter-Glo after 72 hours of drug treatment. Mean and SEM shown for three replicates.

(B) Western blots of pERK and multiple downstream MAPK effector pathways from A375 parental and reversibly resistant cells. Cells were grown off of drug for 24 hours, then with drug added for 4 hours, and lysed. GAPDH served as control.

(C) Schematic of a pharmacological synthetic lethal screen to identify mediators of resistance to the BRAF and MEK combination.

(D) Screening hits are visualized by plotting the function y = the IC50 ratios of either A375 parental treated with drug X/dual resistant cells treated with drug X plus the BRAF and MEK combination (left hand panel) or A375 dual resistant cells treated with X/ dual resistant cells treated with drug X plus the BRAF and MEK combination (right hand panel), x=compounds. The representative candidate compounds are indicated.

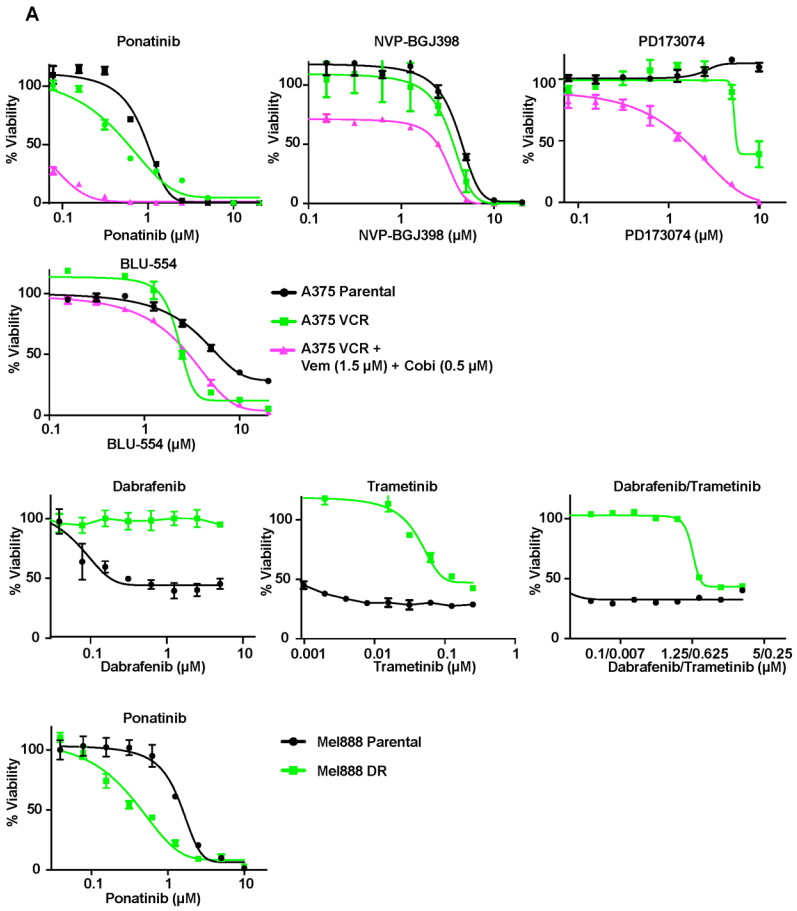

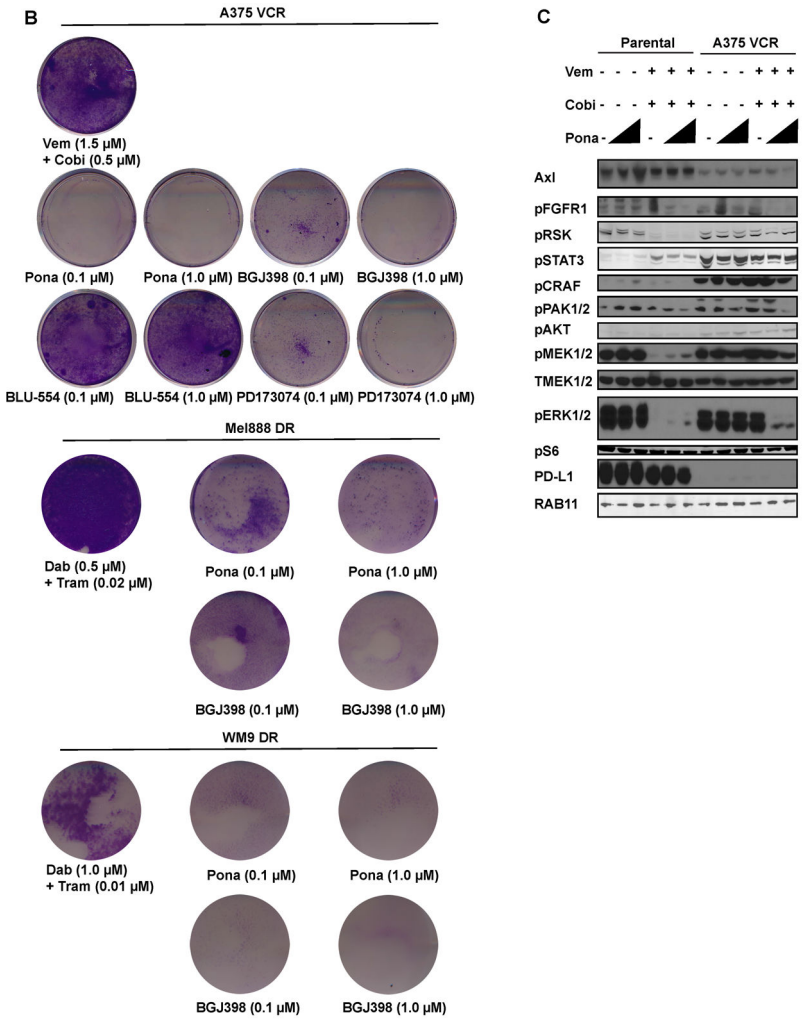

Figure 2. FGFR inhibition synergizes with dual BRAF and MEK inhibition to enhance tumor killing through suppression of pERK.

(A) Top panel: Viability of A375 cells with various FGFR inhibitors in the presence of BRAF and MEK inhibitors, as quantitated by CellTiter-Glo after 72 hours of drug treatment. Bottom panel: Viability of Mel888 parental and dual resistant cells to BRAF and MEK inhibitors as well as to ponatinib. Viability at zero concentration for a given drug is normalized to be one hundred percent. Mean and SEM are shown for three replicates.

(B) Colony formation assay with various FGFR inhibitors. BLU-554 is a FGFR4 selective inhibitor. Vemurafenib (1.5 μM) and cobimetinib (0.5 μM) treated A375 VCR cells served as baseline control. Two different concentrations of each inhibitor (ponatinib, NVP-BGJ398, and BLU-554), 0.1 and 1 μM, were tested in conjunction with vemurafenib and cobimetinib. A375 VCR cells were grown for 21 days and then stained with crystal violet. Mel888 DR cells were treated with dabrafenib (0.5 μM) and trametinib (0.02 μM), plus either ponatinib or NVP-BGJ398 at 0.1 and 1 μM for 9 days. WM9 DR were treated with dabrafenib (1.0 μM) and trametinib (0.01 μM), plus either ponatinib or NVP-BGJ398 at 0.1 and 1 μM for 10 days. Media was changed with fresh drug weekly.

(C) Western blots of A375 parental and reversibly resistant A375-VCR cells treated with ponatinib in combination with dual BRAF/MEK inhibition. Cells were grown off of drug for 24 hours, then with drug added for 4 hours, and lysed. GAPDH served as control.

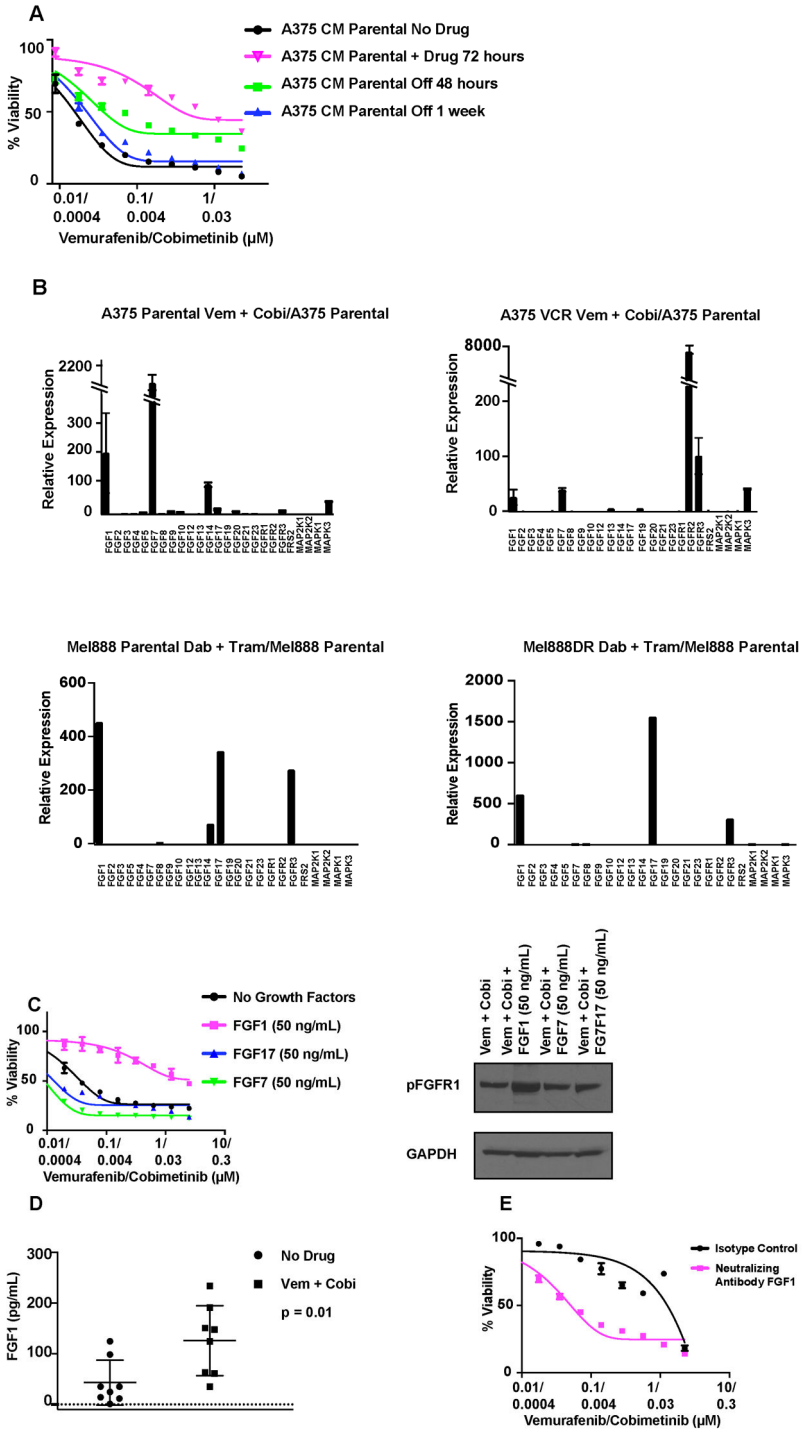

Figure 3. Conditioned media from drug treated cells confers drug resistance to BRAF and MEK inhibitors.

(A) Conditioned media was collected from A375 parental cells (initial plating 1×10^6 million cells) treated with vehicle or vemurafenib (0.1 μM) and cobimetinib (0.01 μM) combination for 72 hours respectively. Fresh drug-free media was exchanged and the supernatant collected at 48 hours and 7 days later. Each conditioned media was mixed with

fresh media in 2:1 ratio and used to culture A375 cells naïve to the BRAF and MEK combination. The cells were treated for 72 hours with titration of the drug combination. Cell viability was quantitated by CellTiter-Glo after 72 hours of drug treatment. Mean and SEM are shown for three replicates.

(B) Transcriptional profiling of FGF pathway using TaqMan real-time PCR assay. Top panel: A375 parental cells were treated with vemurafenib (0.1 μM) and cobimetinib (0.01 μM) for 72 hours. A375 VCR dual resistant cells were treated with vemurafenib (1.5 μM) and cobimetinib (0.5 μM) for 72 hours and compared to the parental line without drug treatment. Mean and SEM are shown for three replicates. Bottom panel: Mel888 parental and dual resistant cells were both treated with dabrafenib (0.5 μM) and trametinib (0.02 μM) for 72 hours prior to RNA extraction. In all cases, gene expression is normalized to that of the parental cells without drug treatment.

(C) Cellular survival of A375 parental cells treated with exogenous hFGFs and combined BRAF/MEK inhibitors for 72 hours was quantitated by CellTiter-Glo. Mean and SEM are shown for three replicates. Western blot of pFGFR1 with GAPDH as control.

(D) ELISA was used to detect hFGF1 from supernatants of vehicle versus drug treated A375 parental cells.

(E) Cellular survival of A375 parental cells treated either with a rabbit polyclonal FGF1 specific antibody (pink) or isotype control (black) and BRAF/MEK combination for 72 hours was quantitated by CellTiter-Glo. Mean and SEM are shown for three replicates.

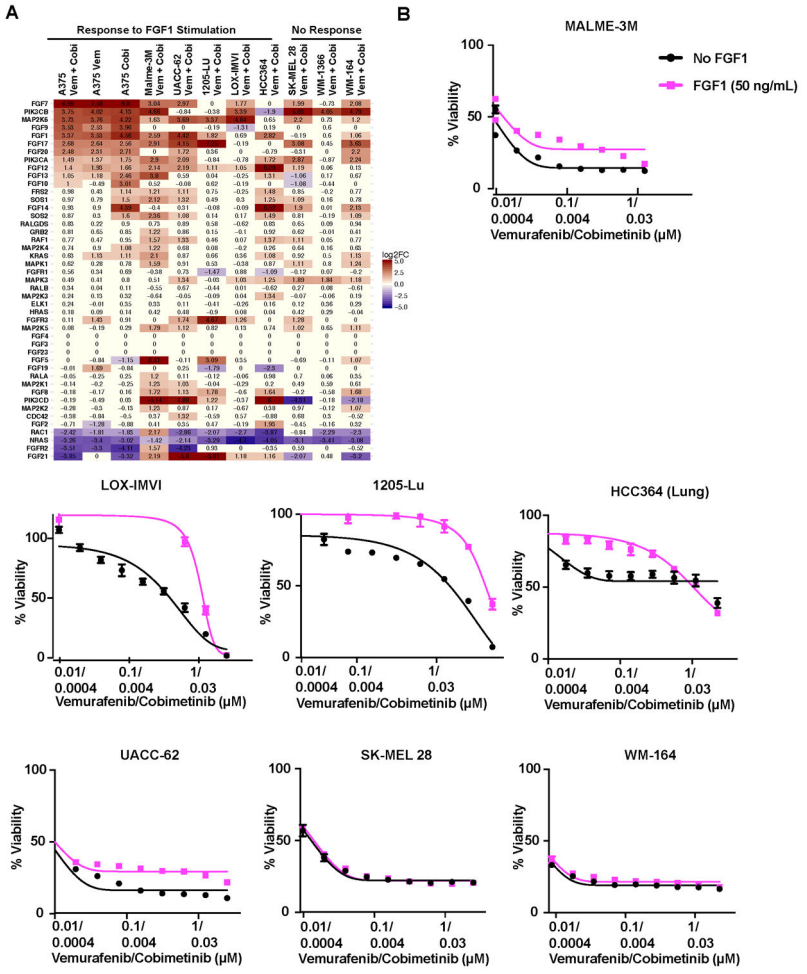

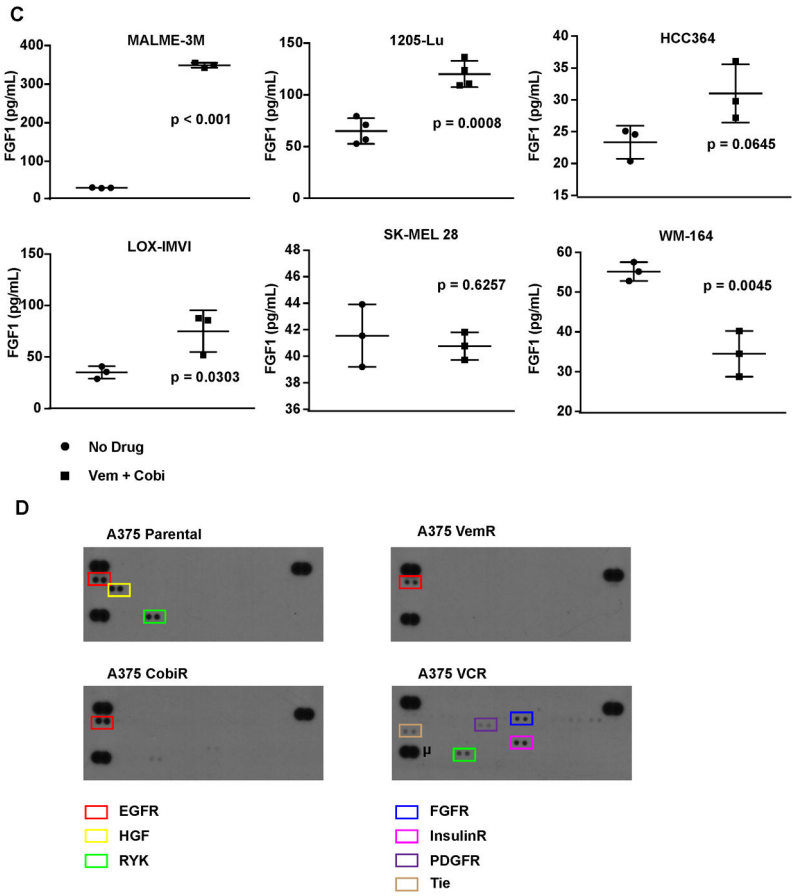

Figure 4. BRAF^{V600E} driven tumor cells transcriptionally upregulate FGF1 in response to dual BRAF and MEK inhibition.

(A) Results of a customized TaqMan human FGF pathway array (Thermo Fischer Scientific). Differential expression change comparing cells treated with vemurafenib and cobimetinib for 72 hours versus the same cell line treated with vehicle calculated using the ΔΔCt method. Data represented average of three TaqMan experiments and the log 2 fold change was plotted.

(B) Cellular survival of various BRAF^{V600E} driven tumor cell lines treated with exogenous hFGF1 and BRAF/MEK inhibitor combination for 72 hours was quantitated by CellTiter-Glo. Mean and SEM are shown for three replicates.

(C) ELISA to assay for hFGF1 in supernatant collected from several BRAF^{V600E} driven tumor cell lines treated with either vehicle or BRAF/MEK combination for 72 hours.

(D) Phospho-RTK arrays from A375 parental, VemR, CobiR, and VCR cells.

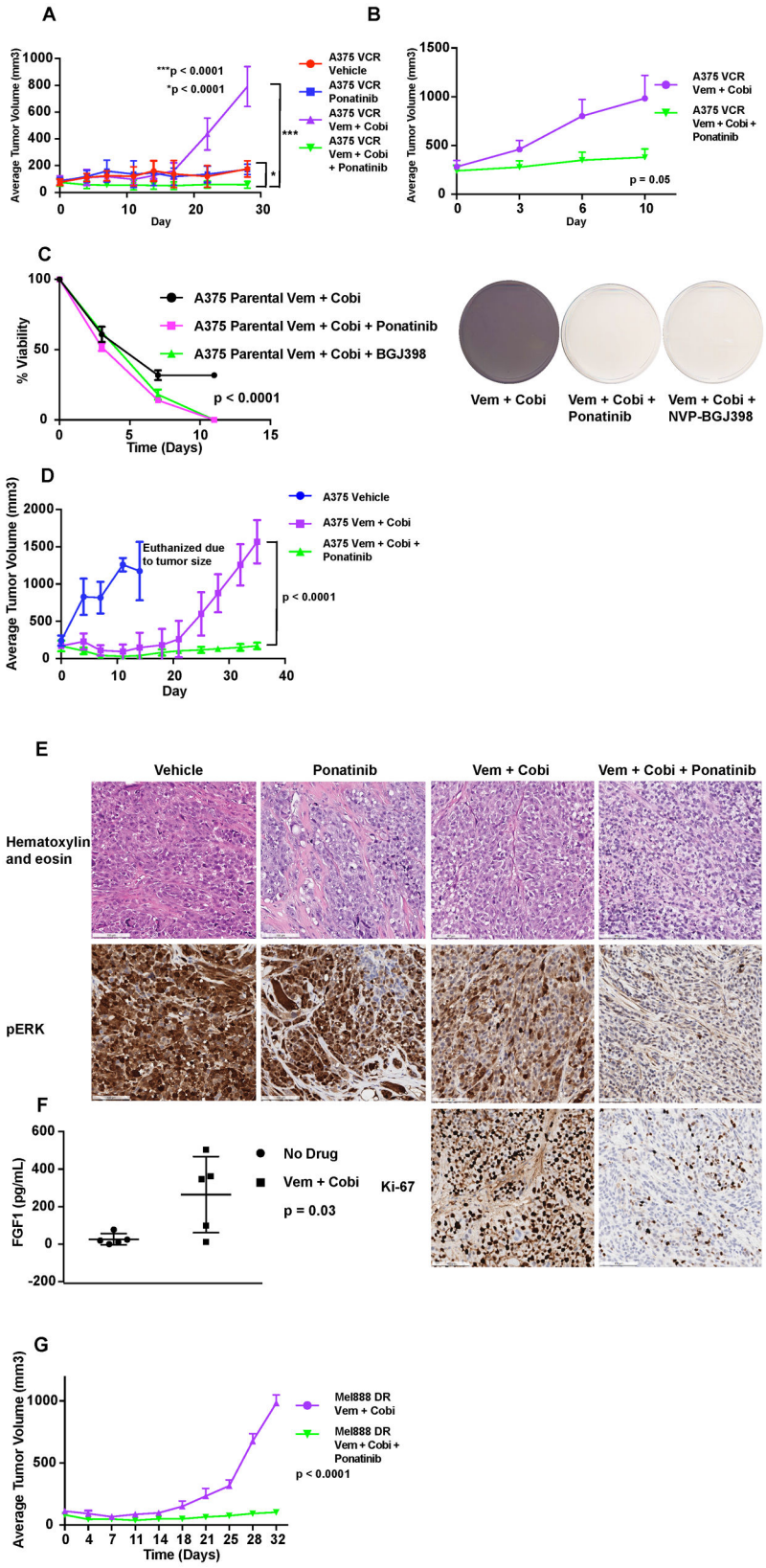

Figure 5. FGFR inhibition in combination of dual BRAF and MEK inhibition induces tumor regression in xenograft models.

(A) Mice bearing the dual resistant A375 VCR cells were treated via oral gavage with the indicated drugs for 28 days (vemurafenib at 25 mg/kg, cobimetinib at 4 mg/kg, and ponatinib at 20 mg/kg). *** comparing the double versus the triple combination. * comparing either vehicle or ponatinib alone versus the triple combination. Error bars represent mean and SEM. p value was calculated using the unpaired t test.

(B) Mice treated with the dual vemurafenib and cobimetinib combination from A were re-randomized either to continue receiving the combination at the same dose or incorporating ponatinib at 20 mg/kg for an additional 11 days. Error bars represent mean and SEM. p value calculated using the unpaired t test.

(C) Cell viability and colony formation assay using the triple combination of BRAF, MEK and FGFR inhibition on the A375 cells. Vemurafenib concentration used was 0.1 μM, cobimetinib 0.01 μM, and ponatinib and NVP-BGJ398 0.1 μM and 0.5 μM respectively. 5×10^5 cells were seeded initially. Media was changed with fresh drug every 3-4 days and total cells remaining were counted at each time point using the Countess II automated cell counter with trypan blue exclusion. Mean and SEM are shown for three replicates.

(D) Mice bearing tumors from the A375 parental cells were grouped and treated with vehicle, vemurafenib (25 mg/kg) and cobimetinib (4 mg/kg), or the triple combination (addition of ponatinib at 20 mg/kg) for 35 days. Error bars represent mean and SEM. p value was calculated using the unpaired t test.

(E) Immunohistochemistry cross section of dual resistant A375 xenograft tumors stained with hematoxylin and eosin, pERK, and Ki-67. The mice were treated with vehicle, ponatinib, vemurafenib and cobimetinib, or the triple combination as indicated in C 4 hours prior to tumor harvesting.

(F) Serum was collected from A375 parental cells tumor bearing mice at baseline and after treatment with vemurafenib and cobimetinib daily for 96 hours. Serum was diluted 1:2 before running ELISA to quantitate the level of hFGF1.

(G) Mice bearing tumors from the Mel888 DR cells were treated with either vemurafenib (25 mg/kg) and cobimetinib (4 mg/kg), or the triple combination (addition of ponatinib at 20 mg/kg) for 32 days. Error bars represent mean and SEM. p value was calculated using the unpaired t test and adjusted for multiple comparisons.

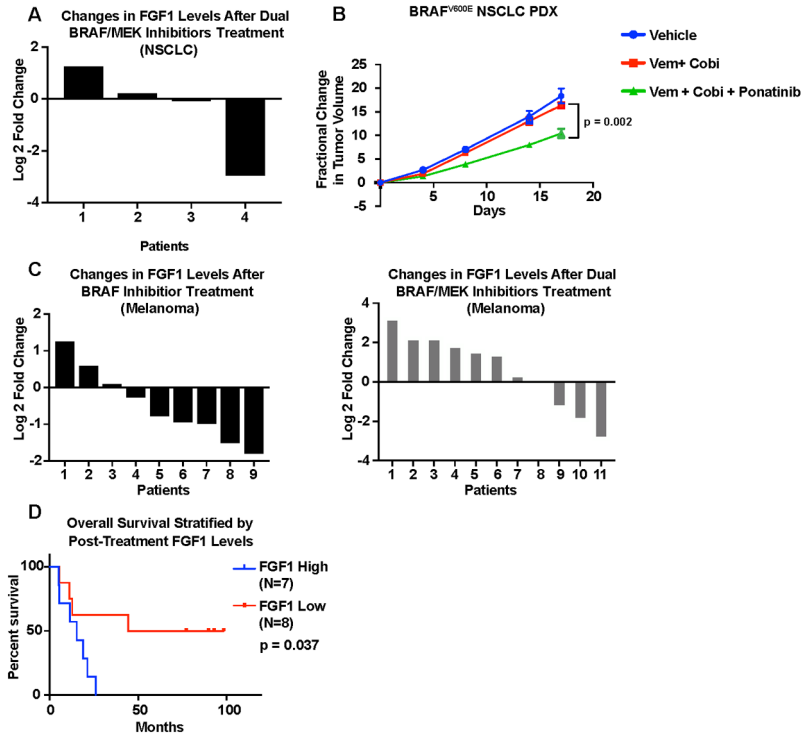

Figure 6. FGF1 mRNA is increased in BRAF^{V600E} patient samples at progression and portends a worse prognosis.

(A) Plot represents log2 fold changes of progression/pre-treatment non-small cell lung cancer samples based on normalized RNA sequencing results for FGF1.

(B) Patient derived xenograft model from a patient with BRAF^{V600E} NSCLC treated with dabrafenib and trametinib combination. Mice were grouped and treated with vehicle, vemurafenib (25 mg/kg) and cobimetinib (4 mg/kg), or the triple combination (addition of ponatinib at 20 mg/kg) for 17 days. Error bars represent mean and SEM. p value was calculated using the unpaired t test.

(C) Plot represents log2 fold changes of post-treatment/pre-treatment melanoma samples based on normalized RNA sequencing results for FGF1. The left hand panel represents patients who were treated with a BRAF inhibitor. The right hand panel consists of patients receiving dual BRAF and MEK inhibitors.

(D) Kaplan-Meier analysis of overall survival for melanoma patients (N=20), stratified by intratumoral FGF1 levels. p value was calculated using the log-rank (Mantel-Cox) test.